



Proton Conductivity Amelioration of Sulfonated Poly Ether Sulfone Octyl Sulfonamide via the Incorporation of Montmorillonite

W. Mabrouk¹ · K. Charradi² · H. Maghraoui-Meherzi³ · A. Alhussein⁴ · Sherif M. A. S. Keshk²

Received: 4 April 2022 / Accepted: 29 July 2022 / Published online: 23 August 2022
© The Minerals, Metals & Materials Society 2022

Abstract

An electrolytic membrane for fuel cell application was fabricated by blending sulfonated poly ether sulfone octyl sulfonamide (SPESOS) with montmorillonite (MMT) clay at different proportions (1 wt.%, 3 wt.%, and 6 wt.%). The structural functionality, surface morphology, and thermal stability of the resultant composite membranes were characterized using Fourier transform infrared spectroscopy, x-ray diffraction, scanning electron microscopy, and thermogravimetric analysis. Interestingly, the thermal properties of the composite membranes were improved compared to pristine SPESOS. Furthermore, proportions as low as 0.1 wt.% in the MMT/SPESOS composite membrane showed superior proton conductivity to the SPESOS membrane. Thus, we propose the MMT/SPESOS composite membrane as a promising material for the electrolytic membrane in fuel cells at temperatures above 100°C.

Keywords SPESOS membrane · ion conductivity · montmorillonite · composite membrane

Introduction

Fuel cells have emerged in recent times as a promising innovation to address the global electric power demand. In contrast to traditional energy generation technologies, fuel cells operate without ignition, thus reducing the harmful ecological impact. Fuel cells act as a continuous source of electrical energy similar to constantly fueled batteries and generate direct current (DC) by utilizing an electrochemical cycle.¹ Among the various types of power modules, those with a polymer electrolyte layer (PEM) have gained increased attention nowadays, for

example, hydrogen power modules, direct methanol energy components, and natural power devices.^{2–4} These power devices operate at room temperature and can generate significant power density. There are several inherent advantages and disadvantages in all designs, all of which however can be limited to some extent by the use of proton-conducting polymeric films. PEM serves as a fuel separator by providing protonic correspondence between the anode and cathode.⁵ Despite several drawbacks, poly(perfluoro alkyl sulfonic acids) like Nafion[®] and similar materials are still the standard film materials for polymer electrolyte fuel cells (PEMFCs). The limitations of these polymers and the interest in innovative and clean energy sources or the creation of good frameworks have led to the search for alternative materials for PEMFCs.⁶ Many promising polymers depend on polyaromatic thermoplastics, for example, poly(aryl ether ketone) (PAEK/PEEK), poly ether sulfone (PES), and polybenzimidazole (PBI), all of which have high rigidity and thermal stability, low cost, and simple handling.^{7–10} The functionalization of these polymers by sulfonation prompts improved layer properties such as better wettability, higher water transition, and better perm selectivity, making sulfonated polymers an excellent candidate for PEMFCs. Another approach to investigate the alternatives for polymer composites in fabricating the best membranes is to utilize functionalized polymers either alone or blended with other polymers or nanoparticles or clay.^{3,4,11–15} Among these

✉ W. Mabrouk
w.mabroukcerte@gmail.com

¹ Laboratory Water, Membranes and Biotechnology of the Environment, CERTE, 8020 Soliman, Tunisia

² Nanomaterials and Systems for Renewable Energy Laboratory, Research and Technology Center of Energy, CRTEn, Technopark Borj Cedria, BP 095, Hammam Lif, Tunisia

³ FST, Laboratory of Analytical Chemistry and Electrochemistry, LR99ES15, University of Tunis El Manar, Campus, 2092 Tunis, Tunisia

⁴ LASMIS Research Unit, Technological Pole of South Champagne, University of Technology of Troyes, Lavoisier rd, 52800 Nogent, France

derivatives, sulfonated poly ether sulfone octyl sulfonamide (SPESOS) exhibits a smooth membrane with varying ionic conductivity and water uptake depending on the amount of grafted octylamine.¹¹ On the other hand, clay minerals have been explored as significant additives to conductive polymers. Clay/polymer composites membrane is expected to show more dimensional stability and consequently stronger polymer/electrode interfaces, thus improving the fuel cell durability.^{3,4,16} Montmorillonite (MMT) is one of the most abundant natural clays with water retention, intercalation, and ion exchange properties.^{17–19} The introduction of MMT onto the polymer matrix enhances a variety of membrane characteristics, such as water uptake, proton conductivity, and mechanical and chemical stability at a high-temperature range.²⁰ In addition, the presence of clay minerals on the surface of the polymeric membrane is beneficial for fuel cell performance.²¹ The increased proton conductivity due to the introduction of clay minerals is attributed to the water retention ability of clay layers, resulting in the superior performance of membranes even at higher temperatures by preventing dehydration.²² The presence of water linked with clay minerals favors proton transport (a vehicular mechanism) and plays a vital role in improving proton conductivity. The MMT clay/poly(ether ether ketone) composite showed improved characteristics including 2.4 meq/g ion exchange capacity, 75% water uptake, and 0.06 S/cm proton conductivity.⁵ A nanocomposite film with a sandwich-like structure was prepared by intercalating conductive polyaniline (PANi) into the interlayer of MMT with a layered structure for quick and selective separation of Pb²⁺ ions.²³ This MMT/PANi nanocomposite film exhibited an ion exchange capacity as high as 213.4 mg g⁻¹ and maintained above 90% of its initial ion exchange capacity even after 20 repeated cycles of Pb²⁺ ion uptake analysis. In the present study, SPESOS was used as an electrolyte matrix. Furthermore, MMT/SPESOS composite with various clay ratios was prepared by the solution casting method for the first time to increase the conductivity of the resulting SPESOS membrane. The physicochemical characterizations of the composite membranes were investigated via Fourier transform infrared (FT-IR) spectroscopy, x-ray diffraction (XRD), scanning electron microscopy (SEM), and thermogravimetric analysis (TGA). Furthermore, the proton conductivity (up to 100°C) and water uptake of the composite membranes were evaluated.

Materials and Methods

Materials

The authors synthesized sulfonated poly ether sulfone octyl sulfonamide (SPESOS) in ERAS Labo.¹ Montmorillonite (MMT) is a soft phyllosilicate mineral, and it contains hydrated sodium calcium aluminum magnesium silicate

hydroxide (Na, Ca)_{0.33}(Al, Mg)₂(Si₄O₁₀) (OH)₂nH₂O. *N,N'*-dimethylacetamide (DMAc) was purchased from Acros. Sulfuric acid was purchased from Scharlau, and sodium hydroxide was purchased from Laurylab.

Membrane SPESOS Preparation

A calculated amount of powdered sulfonated SPESOS was dissolved in dimethylacetamide (DMAc) for 15 min and magnetically stirred at room temperature to obtain a 10% solution in mass of SPESOS.²⁶ After stirring, a transparent homogeneous polymer solution was obtained. Then, the polymer solution was cast on smooth Teflon[®] support and distributed homogeneously and was dried in an oven under different conditions of 50°C for 12 h, 80°C for 6 h, and 100°C for 12 h.¹¹ The fabrication of the membranes was carried out using three temperatures stages: the first stage (50°C for 12 h) to evaporate the maximum amount of solvent and avoid the formation of air bubbles in the membrane; the second stage (80°C for 6 h) to obtain a viscous solution and uniform thickness of the membrane; and finally, the last stage (100°C for 12 h) to evaporate the solvent residual from the formed membranes. After the sample was cooled, the reference SPESOS membrane was wetted with distilled water and removed from the Teflon[®]. The obtained membrane was stored in a moist environment.

Composite Membrane Preparation

The solution dispersion technique and the casting evaporation method were combined to produce the composite membranes. Dispersions composed of varying MMT content (1, 3, and 6 mass%) and SPESOS (10 mass%) were prepared. Initially, different quantities of MMT powder were dissolved separately in 5 mL DMAc under magnetic stirring at room temperature for 2 days. The resultant solutions were subjected to ultrasonication for 4 h to obtain a uniform dispersion of the filler. Finally, each MMT solution was added to SPESOS (10 mass%) polymer solution. The resulting polymer solutions were magnetically stirred for 2 h. The dispersion solutions were spread on the Teflon[®] support (surface 10 × 10 cm) and distributed evenly. The samples were then subjected to drying under different conditions. The thickness of all the elaborated membranes was around 100 μm.

Characterization

FT-IR analysis was performed in transmission mode using a Nicolet spectrophotometer (IR200 FT-IR). The spectra of SPESOS and the different composite membranes were

measured on the page from 400 to 4000 cm^{-1} . The membrane samples were placed between the cast iron and the diamond crystal (separator blade) without any pretreatment for recording the spectra.

An automated Bruker D8 Advance x-ray diffractometer was used to evaluate x-ray diffractograms in the 2-theta range of 5° – 60° . The dry composite membrane samples were analyzed without any pretreatment. The crystalline size of the SPESOS and its composites were determined by the x-ray line broadening method using the Scherrer equation $D = (k\lambda/\beta_D \cos\theta)$, where D is the crystalline size in nanometers, λ is the wavelength of the radiation (1.54056 Å for $\text{CuK}\beta$ radiation), k is a constant equal to 0.94, β_D is the peak width at half-maximum intensity, and θ is the peak position.

Thermogravimetric analysis (TGA) was carried out using a Mettler Toledo thermogravimetric analyzer. Approximately 2.5 mg and 3.5 mg of membrane samples were first dried at 100°C for 24 h to remove any moisture and solvent. Then, the software was programmed from 25°C to 900°C at a rate of $10^\circ\text{C}/\text{min}$ under a 40 mL/min nitrogen flow.

Scanning electron microscopy (SEM) was used to observe the surface morphology of the membranes and their cross-section. The membranes were fractured after cooling with liquid nitrogen for this analysis. Observations were made using a Hitachi 4800 II SEM and were made directly on the surface and cross-sections of the samples without any prior treatment.

Dry samples were employed to determine the water uptake (WU). Water uptake measurements were made after soaking each membrane in deionized water for 72 h at room temperature, and the wet weight was recorded after removing the surface water with hydrophilic paper.²⁴ From the difference in mass before and after absorption of water by the membrane, WU values were calculated as the relative weight gain per gram of the dry sample using the following Eq. 1:

$$\text{WU} = \frac{W_{\text{wet}} - W_{\text{dry}}}{W_{\text{dry}}} * 100 \quad (1)$$

where W_{wet} and W_{dry} are the weight of the wet and dry membranes, respectively.

The contact angle (CA) of the different membranes was determined using a Theta optical tensiometer (Attension). As such, a photo of the droplet of demineralized water (5 μL) deposited on the membrane was recorded by a camera, and CA was calculated using the computer software Theta (Attension).²⁵

The ionic exchange capacity (IEC) was determined by acid-basic titration. The different proton exchange membranes (area = $5 \times 5 \text{ cm}^2$) were immersed separately for 2 days in sodium hydroxide aqueous solution (100 mL, 10^{-2} M). This period of time is necessary for the exchange of the sulfonated groups (SO_3H) of the membranes to be

transformed into groups (SO_3Na). The protons of the sulfonated groups released in the solution are neutralized by the OH^- ions to form water. Finally, the initial solution and the NaOH solution were titrated with aqueous solutions of sulfonic acid.^{26–28} The IEC for each membrane was calculated by the following relation:

$$\text{IEC} = \frac{n_{\text{NaOH}}^i - n_{\text{NaOH}}^f}{W_{\text{dry}}} \quad (2)$$

where n_{NaOH}^i is the initial mol number of sodium hydroxide in solution (10^{-2} M , 200 mL), n_{NaOH}^f is the mol amount of sodium hydroxide after exchange and W_{dry} is the dry mass of the membrane.

The proton conductivity of the prepared membranes as a function of temperature and the amount of MMT added was measured by EIS (electrochemical impedance spectroscopy) using a Biologic Science Instruments VSP potentiostat. The electrical resistance (R) of the different membranes was determined by the intersection of the layout of the high-frequency Nyquist diagrams and the abscissa axis using ZView software.²⁹ Ionic conductivity (σ , mS/cm) was calculated using the following relation:

$$\sigma (\text{mS}/\text{cm}) = \frac{e}{R \times S} \quad (3)$$

where e denotes the thickness and S is the surface of the membrane placed between the two electrodes and R is the electrical resistance.

Results and Discussion

The FT-IR spectrum of the MMT/SPESOS membrane at varying concentrations, along with spectral observations of MMT and SPESOS individually, is presented in Fig. 1.

The FT-IR spectra of MMT revealed characteristic peaks at 3395 & 3637 cm^{-1} corresponding to the stretching vibrations of O-H and at 1123–1023 cm^{-1} to the stretching vibrations of Si-O. Additionally, a characteristic bending vibration of the Si-O bond at 520 cm^{-1} was also evidenced.³⁰ On the other hand, the characteristic bands of SPESOS at 1482 and 1590 cm^{-1} correspond to the aromatic carbons, and that at 1005 and 1074 cm^{-1} can be ascribed to the symmetric and asymmetric stretching vibrations of the O=S=O group of the sulfonic acid (Fig. 1).³¹ The absorption band present between 2750 and 3000 cm^{-1} is associated with stretching vibrations of CH_2 group.³¹ However, the spectra of the MMT/SPESOS (c, d, and e) composite membranes depict the characteristic bands belonging to MMT and SPESOS along with several new absorption bands. The peaks at 3458 cm^{-1} and 1630 cm^{-1} assigned to stretching vibrations

of the O-H from water molecules and that at 2950 cm^{-1} is due to C-H stretching vibrations (Fig. 1).

The MMT/SPESOS composite has reduced intensity of -OH stretching bond vibration of pristine MMT, as a

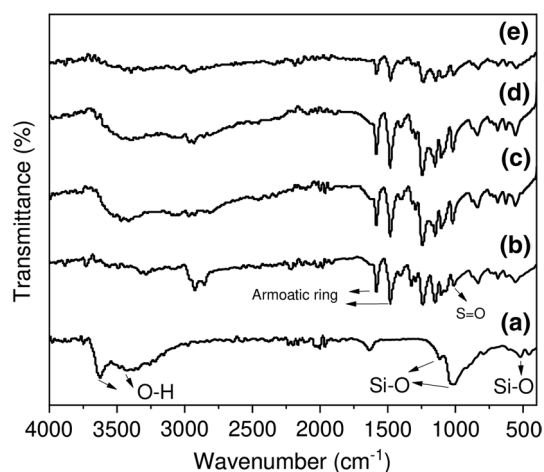
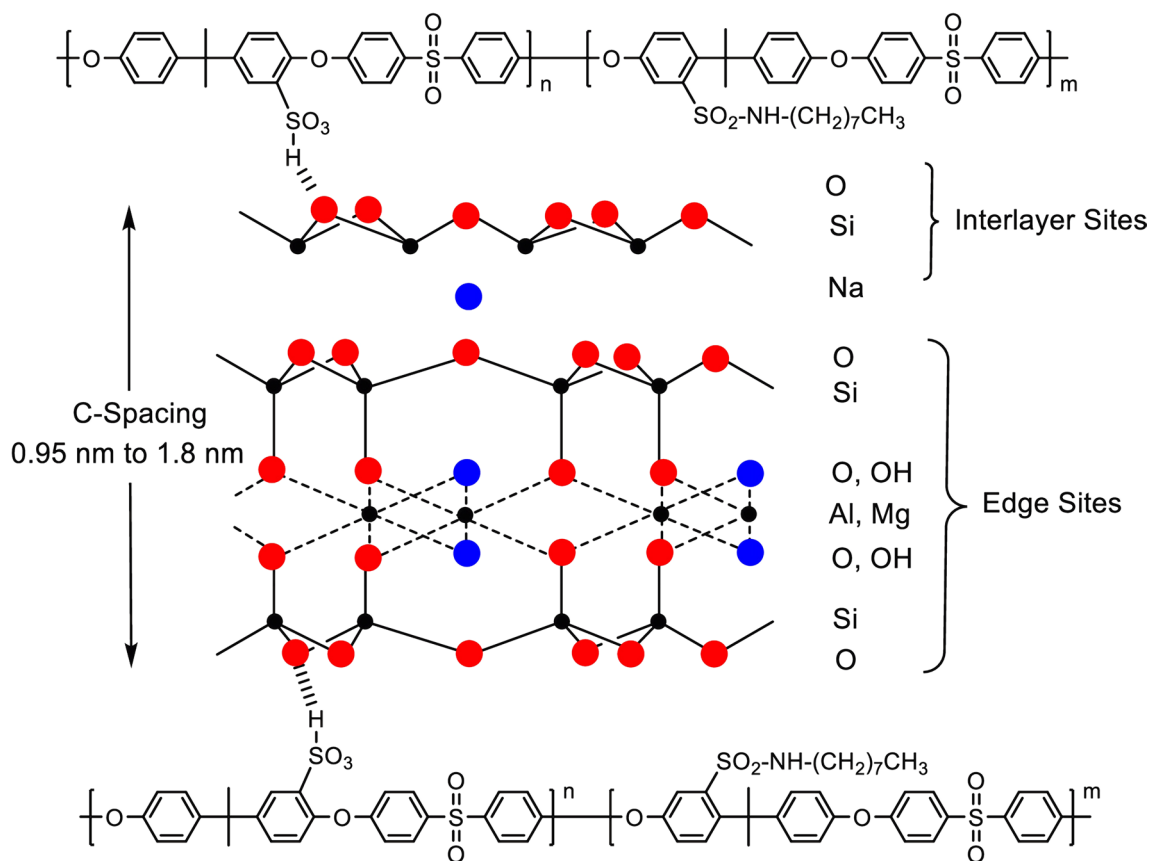


Fig. 1 FT-IR spectra of (a) MMT, (b) SPESOS, (c) 1% MMT/SPESOS, (d) 3% MMT/SPESOS and (e) 6% MMT/SPESOS composite membranes.

result of the consumption of the MMT hydroxyl groups via interaction with SPESOS, while the surface of the MMT showed decreasing water adsorption. In addition, the observed effect of MMT on SPESOS structure around 1020 cm^{-1} and 560 cm^{-1} may be attributed to Si-O vibrations originating from MMT introduction (Fig. 1) and signifies the interactions between the SPESOS matrix and the MMT phase. The SO_3H groups and SO_2 groups of SPESOS may interact with Si-O-Si groups of the silicate layer of MMT (Scheme 1).

Unfortunately, the strong change in the Si-O-Si absorbance band was not observed in this case because of the overlapping of the Si-O-Si absorbance band with SPESOS bands. Further, it can be observed that there is only one OH stretching peak at 3458 cm^{-1} in the composite membrane, unlike MMT. Moreover, the peak shifted to the lower wavenumbers. This can be attributed to the formation of new hydrogen bonds between the SPESOS molecules and MMT during the preparation of the composite. Figure 2 presents the XRD diffractograms of all the samples. The major peaks at $2\theta = 11.66^\circ, 29.34^\circ, 35.93^\circ, 39.34^\circ, 43.25^\circ, 47.46^\circ,$ and 48.51° are observed in all the



Scheme 1 Chemical interaction between the MMT and SPESOS.

diffraction patterns and correspond to the crystallographic planes of the MMT nanoparticles present in membranes.

The interaction of MMT layers with the SPESOS causes the peak at $2\theta = 15.45^\circ$ to shift toward slightly higher 2θ values owing to change in the lattice structure from the linkage between SPESOS and MMT particles that made tension stress (lattice compression) (Fig. 2; Table I).

Furthermore, the d-spacing value decreased after incorporating the MMT (Table I). This may be attributed to the change in crystallite size and different atomic radii confirming that MMT was successfully incorporated. Besides, the appearance of the MMT peaks in the MMT blended SPESOS samples indicates the successful intercalation of the MMT in SPESOS. Thus, the fabrication of organic–inorganic composite membranes results in diverse structures, shapes, and properties of inorganic complementary advantages, demonstrating the synergistic effect and improving the comprehensive properties of the composite membranes. SEM analysis is a surface technique to identify the surface morphology of the prepared composites, and the analysis can effectively track the minute cracks or fractures in the membrane. The SEM images of all the composite membranes are presented in Fig. 3.

The micrographs in Fig. 3 confirm the homogeneity of the fabricated composite membranes by the absence of cracks, holes, and pores. It can be inferred that the in situ polymerization method of fabrication of composite membranes can reliably produce evenly distributed membranes. The

SPESOS molecular chains aggregate to form a domain structure, and MMT nanoparticles are embedded in the SPESOS matrix.

The drop shape analysis method can be used to determine the surface properties of SPESOS that change during the process of MMT incorporation (Fig. 4). The contact angle analysis provides insight into the super wettability of the materials concerning the composite areas. The hydrophilic/hydrophobic properties of the composite can be controlled by adjusting the tangent between the surface of the sessile drop and the contact outline formed with the surface (Fig. 4). The contact angle values of the various membranes are less than 90° , confirming that these prepared membranes have sufficient hydrophilicity. The introduction of MMT decreased the contact angle values, indicating improved hydrophilicity. It can be seen from the thermogravimetric analysis (TGA) of the different

Table I XRD analysis of SPESOS and MMT/SPESOS composite membranes

Sample	2θ ($^\circ$)	d (001) Å
SPESOS	15.45	5.73
1% MMT/SPESOS	18.35	4.83
3% MMT/SPESOS	18.39	4.82
6% MMT/SPESOS	18.02	4.91

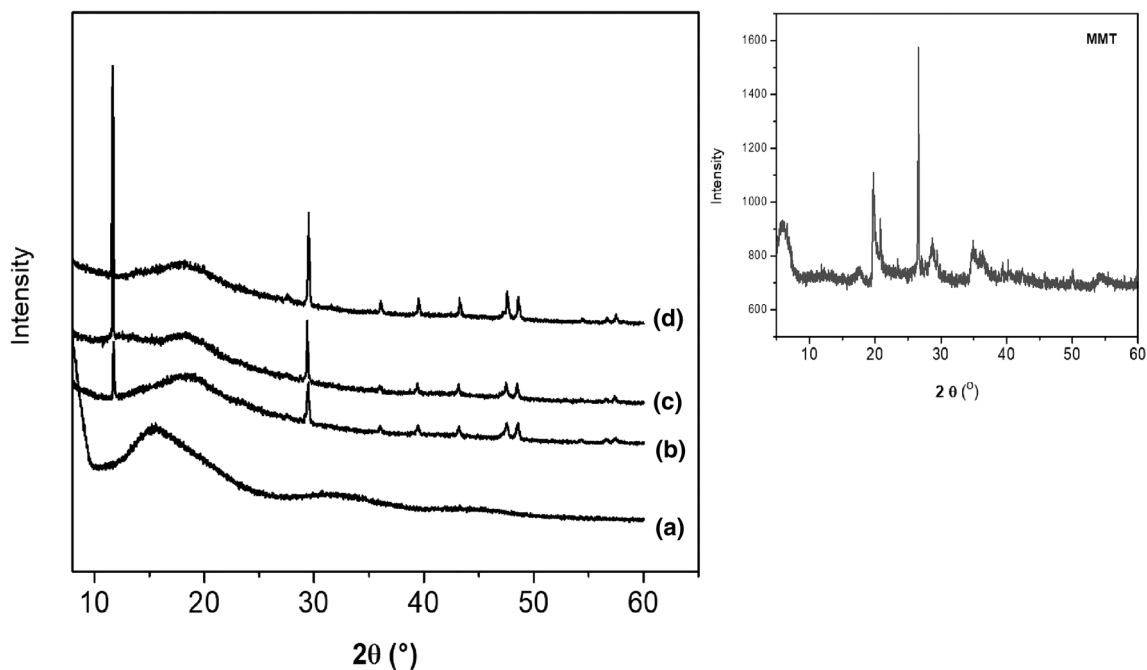


Fig. 2 X-ray diffraction patterns of MMT, (a) SPESOS, (b) 1% MMT/SPESOS, (c) 3% MMT/SPESOS, and (d) 6% MMT/SPESOS composite membranes.

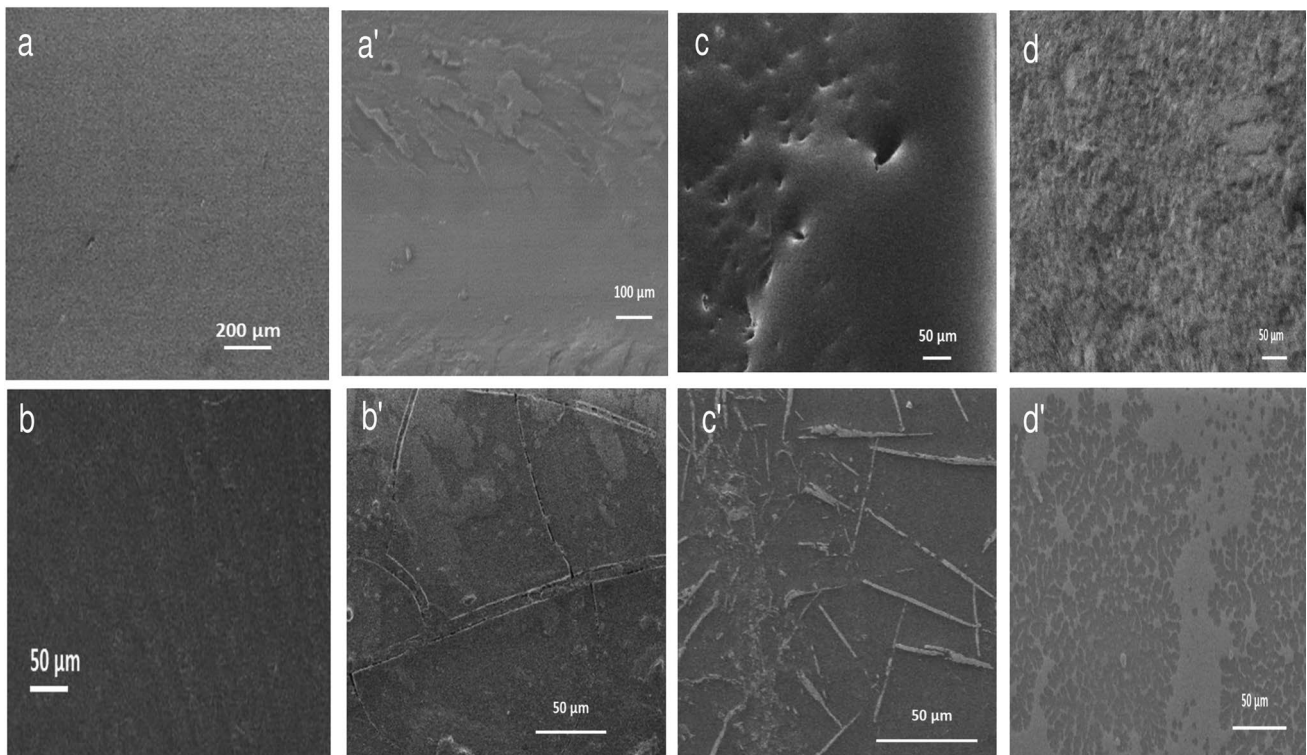


Fig. 3 SEM micrograph of the membrane surfaces (a) SPEOS, (b) 1% MMT/SPEOS, (c) 3% MMT/SPEOS, (d) 6% MMT/SPEOS, and cross section (a') SPEOS, (b') 1% MMT/SPEOS, (c') 3% MMT/SPEOS and (d') 6% MMT/SPEOS.

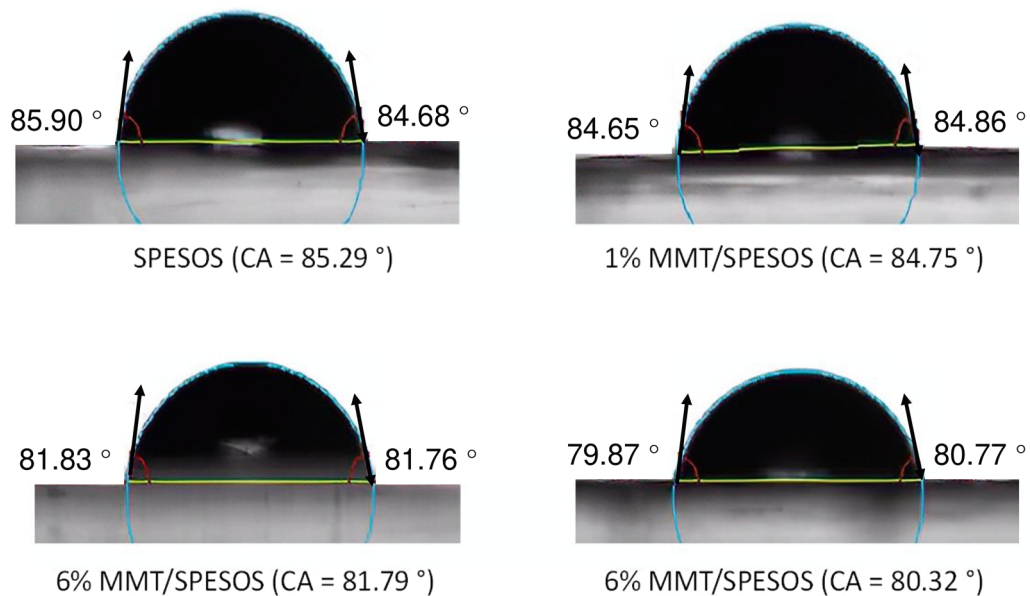


Fig. 4 Contact angle of fabricated composite membranes.

membranes that the various fabricated membranes exhibited somewhat similar behavior without any anomalies (Fig. 5).

The first loss of mass indicated by the thermograms appears around 100°C and corresponds to the evaporation of water from the SPEOS matrix. The second significant

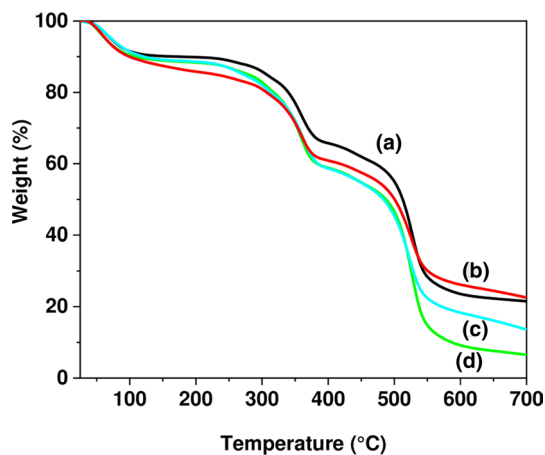


Fig. 5 Thermogravimetric analysis of (a) SPESOS, (b) 1% MMT/SPESOS, (c) 3% MMT/SPESOS, and (d) 6% MMT/SPESOS composite membranes.

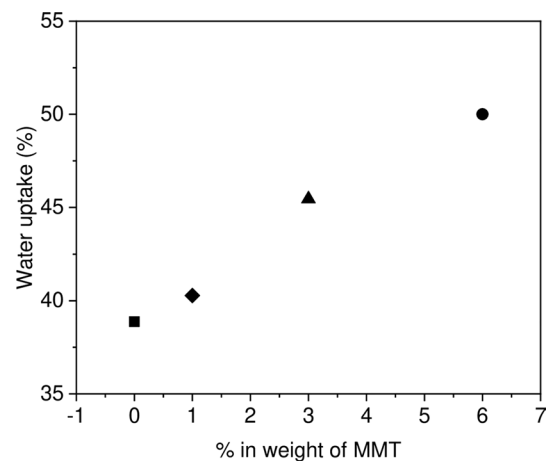


Fig. 6 Water uptake statistics of the composite membrane with increasing MMT percentage in the virgin SPESOS membrane. (■) SPESOS, (◆) 1% MMT/SPESOS, (▲) 3% MMT/SPESOS and (●) 6% MMT/SPESOS composite membranes.

Table II Comparison between experimental and theoretical values of ion exchange capacity of all as-prepared membranes

Membrane	Theoretical ion exchange capacity/ (meq/g)	Experimental ion exchange capacity/ (meq/g)
SPESOS	2.00	1.94
1% MMT/SPESOS	2.00	1.93
3% MMT/SPESOS	2.00	1.95
6% MMT/SPESOS	2.00	2.15

mass loss is observed at around 300°C and is attributed to the deterioration of the sulfonic groups, followed by a final mass loss at around 500°C owing to the decomposition of the main matrix of the SPESOS. Nevertheless, the thermal stability of all the membranes prepared is acceptable for the temperatures corresponding to the proton exchange membrane fuel cell applications.²⁷ Table II shows the values of the theoretical and experimental ion exchange capacities of the manufactured composite membranes with a surface area equal to 25 cm².

The theoretical calculation of ion exchange capacity was carried out in previous¹¹ works which compared the signals of the aromatic protons of the commercial poly ether sulfone and SPESOS obtained by ¹H nuclear magnetic resonance (NMR) spectroscopy. SPESOS indeed gives two peak masses of aromatic protons. The theoretical ion exchange capacity can be obtained from the ratio R of the surfaces of the two masses. The results are consistent with the composition of the membranes, where the SPESOS reference membrane has an ion exchange capacity equal to 2 meq/g. The theoretical capacity did not vary much with the increasing percentage of MMT in the SPESOS matrix.

On the other hand, a slight increase in the experimental ion exchange capacity of the composite membranes, obtained using Eq. 2, is observed when the percentage of MMT in the matrix of the virgin membrane increases. This increase can be explained by the hydrophilic nature of MMT, which facilitates proton exchange through the membrane. The variation between the theoretical and experimental values is acceptable if the experimental errors made during the acid–base assay are considered. Figure 6 reproduces the variation in the water uptake, calculated using Eq. 1, of the composite membranes with that of the SPESOS (2 meq/g) when the percentage of MMT is increased.

The fabricated membranes tend to absorb more water than the reference sample SPESOS (2 meq/g) due to the addition of MMT (Fig. 6). It is worth noting that the water uptake of the composite membranes is significantly higher when the proportion of added MMT is high, which is more likely due to a significant increase in the hydrophilic nature of the SPESOS by added MMT. Indeed, at room temperature, the rate of water uptake of the composite membranes increases from 40 to 50% by mass for the membranes with 1% and 6% of MMT, respectively, while it remains around 38% for the reference sample. These results are in concordance with those observed from the contact angle values. The electrochemical performance based on the ability of protons to migrate through the membrane was studied using AC impedance spectroscopy with 100% relative humidity (RH) from room temperature to 100°C (Fig. 7).

The values of proton conductivity of the different membranes during the increase in temperature were calculated using Eq. 3. The increased proton conductivity of the membranes with temperature is depicted in Fig. 7.

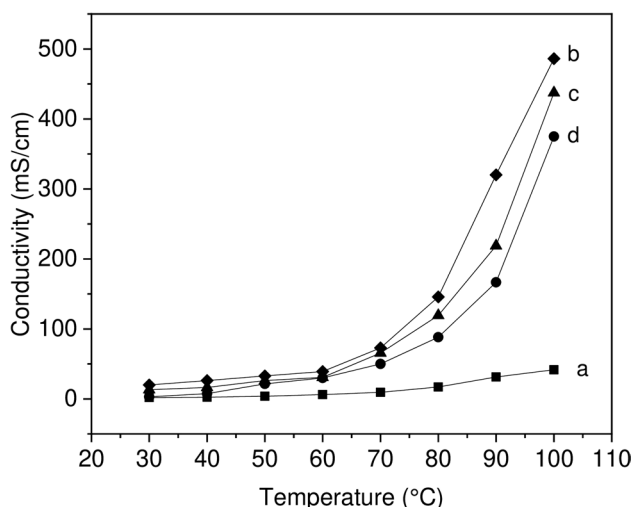


Fig. 7 Evolution of proton conductivity of different composite membranes at 100% relative humidity (a) SPESOS, (b) 1% MMT/SPESOS, (c) 3% MMT/SPESOS, and (d) 6% MMT/SPESOS composite membranes.

At all temperatures, the lowest recorded proton conductivity values were observed for the SPESOS reference membrane. The proton conductivity at 100°C of SPESOS is 41 mS/cm, while those of the nanocomposite membranes containing 1, 3, and 6% by weight of MMT are 486, 437, and 375 mS/cm, respectively. The higher proton conductivity of composite membranes containing different percentages of MMT compared to that of SPESOS can be attributed to the better water retention ability (solvation of proton) at high temperatures (100°C). The water retention factor, in turn, is related to the hydrogen bonds with the hydrophilic groups in the composite membranes (sulfonated groups) and the better affinity of MMT toward water (Scheme 1). However, the proton conductivity (at 100°C) of the composite membranes gradually decreases with the increasing proportion of MMT.

The layered structure and hygroscopic nature of MMT contribute to better water retention at high temperatures.^{33,34} The comportment of the proton conductivity of the membranes at high temperatures has been studied in various works. Let us quote, for example, the proton conductivity of SPEEK at 100°C is 90 mS/cm while those of the nanocomposite membranes containing 1, 3, and 5 wt.% of sulfonated MMT are respectively 105, 100, and 30 mS/cm.³³ The relationship between temperature and proton conductivity can be obtained using the Arrhenius equation.¹⁷ Thus, the activation energy of conductivity can be calculated using the following equation:

$$\sigma = \sigma_0 \exp(-E_a/RT) \quad (4)$$

Table III Activation energy values and proton conductivity at 100°C

Membrane	Conductivity (mS/cm) at 100°C	E_a (kJ/mol)
SPESOS	41.7	36.5
1% MMT/SPESOS	468.1	13.9
3% MMT/SPESOS	437.5	15.5
6% MMT/SPESOS	375.0	24.9

where σ is the proton conductivity (S/cm), σ_0 is the pre-exponential factor, R is the universal gas constant (8.314472 J/mol·K), and T is the absolute temperature (K).

Table III summarizes the activation energies of SPESOS obtained using Eq. 4, and its nanocomposite membranes determined from experiments carried out at 100% RH. The composite membranes show lower values of activation energy than the pristine SPESOS.

It can be observed that the incorporation of the filler influences the E_a , and the lowest value is obtained with 6% of clay. Thus, the MMT in the membrane surface can prevent electric field erosion of the internal structure and improve the corona resistance of composite membranes at high ratios of MMT. These results are in good agreement with the proton conductivity results. The values of E_a increased with the introduction of MMT in the membranes. Correspondingly, the best proton conductivity obtained at 100°C with 6% clay confirmed that the water present in MMT accelerates the proton flow at high temperatures. These conductivity values are higher than that of Nafion® 117 membranes with clay, which is about 120 mS/cm at 100°C.^{32,33}

Conclusion

Montmorillonite/SPESOS composite membranes were fabricated, characterized, and evaluated for their potential as electrolytic membranes in fuel cell applications. The results of the FT-IR and XRD analyses confirmed the successful incorporation of MMT in the SPESOS matrix. The water absorption profiles of the composite membranes increased with increasing clay content. The water uptake value, contact angle, ion exchange values, activation energy, and proton conductivity values of the various samples were investigated in detail. The 1 wt.% MMT composite membrane showed superior proton conductivity performance and reasonably good MMT dispersion among all the studied samples. Therefore, SPESOS/MMT with MMT of 1% by weight showed optimal performance and represents a promising composite material for electrochemical applications. The hydrophilic nature of the MMT phase embedded in SPESOS benefits the composite membrane. It was expected that the incorporation of MMT into the SPESOS matrix would provide excellent

fuel cell performance compared with the bare SPESOS membrane. Thus, the present study can serve as a guide for the fabrication of other composite membranes blended with different nanoparticles such as sepiolite, graphene oxide, and hydroxyapatite.

Acknowledgments The authors extend their appreciation to the manager of ERAS Labo for providing the SPESOS polymer free of charge.

Conflict of interest The authors declare no conflict of interest.

References

- N. Thmaini, K. Charradi, A. Zayarya, P. Aranda, and R. Chtourou, Nafion/SiO₂@TiO₂-Palgorskite Membranes with Improved Proton Conductivity. *J. Appl. Polym. Sci.* 139, e52208 (2022).
- Q.A. Alsulami, L.M. Alharbi, and S.M.A.S. Keshk, Synthesis of a Graphene Oxide/ZnFe₂O₄/Polyaniline Nanocomposite and Its Structural and Electrochemical Characterization for Supercapacitor application. *Int. J. Energy Res.* 46, 2438–2445 (2021).
- Z. Ahmed, Q.A. Alsulami, K. Charradi, S.M.A.S. Keshk, and R. Chtourou, Physicochemical Characterization of Low Sulfonated Polyether Ether Ketone/Smectite Clay Composite For Proton Exchange Membrane Fuel Cells. *J. Appl. Polym. Sci.* 138, 49634–49642 (2021).
- K. Charradi, Z. Ahmed, N. Thmaini, P. Aranda, Y.O. Al-Ghamdi, P. Ocon, S.M.A.S. Keshk, and R. Chtourou, Incorporating of Layered Double Hydroxide/Sepiolite to Improve the Performance of Sulfonated Poly(Ether Ether Ketone) Composite Membranes for Proton Exchange Membrane Fuel Cells. *J. Appl. Polym. Sci.* 138, 50364 (2021).
- M.M. Hasani-Sadrabadi, S.H. Emami, R. Ghaffarian, and H. Moaddel, Nanocomposite Membranes Made from Sulfonated Poly (Ether Ether Ketone) and Montmorillonite Clay For Fuel Cell Applications. *Energ. Fuel* 22, 2539–2542 (2008).
- J. Meier-Haack, C. Vogel, W. Butwilowski, and D. Lehmann, Sulfonated poly(ether sulfone)s for Fuel Cells by Solvent-Free Polymerization. *Pure Appl. Chem.* 79, 2083–2093 (2007).
- J.A. Kerres, Development of Ionomer Membranes for Fuel Cells. *J. Membrane Sci.* 185, 3–27 (2001).
- K.D. Kreuer, On Development of Proton Conducting Polymer Membranes for Hydrogen and Methanol Fuel Cells. *J. Membrane Sci.* 185, 29–39 (2001).
- O. Savadogo, Emerging Membranes for Electrochemical Systems: Part II. High Temperature Composite Membranes for Polymer Electrolyte Fuel Cell (PEFC) Applications. *J. Power Sources* 127, 135–161 (2004).
- M. Rikukawa and K. Sanui, Proton-Conducting Polymer Electrolyte Membranes Based on Hydrocarbon Polymers. *Prog. Polym. Sci.* 25, 1463–1502 (2000).
- W. Mabrouk, L. Ogier, F. Matoussi, C. Sollogoub, S. Vidal, M. Dachraoui, and J.F. Fauvarque, Preparation of New Proton Exchange Membranes Using Sulfonated Poly(Ether Sulfone) Modified by Octylamine (SPESOS). *Mater. Chem. Phys.* 128, 456–463 (2011).
- A.H. Avci, T. Rijnaarts, E. Fontananova, G.D. Profio, I.F.V. Vankelecom, W.M.D. Vos, and E. Curcio, Sulfonated Polyethersulfone Based Cation Exchange Membranes for Reverse Electrodialysis Under High Salinity Gradients. *J. Membrane Sci.* 595, 117585 (2020).
- A. Kraysberg and Y. Ein-Eli, Review of Advanced Materials for Proton Exchange Membrane Fuel Cells. *Energy Fuel* 28, 7303–7330 (2014).
- S.S. Lim, W.R.W. Daud, J.M. Jahim, M. Ghasemi, P.S. Chong, and M. Ismail, Sulfonated Poly(Ether Ether Ketone)/Poly(Ether Sulfone) Composite Membranes as an Alternative Proton Exchange Membrane in Microbial Fuel Cells. *Int. J. Hydrogen Energy* 37, 11409–11424 (2012).
- K. Widhyahrini, N. Handayani, D. Wahyuningrum, and C.L. Radiman, The Synthesis of Sulfonated Polyethersulfone (SPES) and the Preparation of its Membranes as Matrix in the Immobilization of Candida Antartica Lipase B (Cal-B). *Polym. Bull.* 77, 3735–3748 (2020).
- D. Plackett, A. Siu, Q. Li, C. Pan, J.O. Jensen, S.F. Nielsen, A.A. Permyakova, and N.J. Bjerrum, High-temperature Proton Exchange Membranes based on Polybenzimidazole and Clay Composites for Fuel Cells. *J. Membrane Sci.* 383, 78–87 (2011).
- K. Charradi, Z. Ahmed, P. Aranda, and R. Chtourou, Silica/Montmorillonite Nanoarchitectures and Layered Double Hydroxide-SPEEK Based Composite Membranes for Fuel Cells Applications. *Appl. Clay. Sci.* 174, 77–85 (2019).
- M. Chauhan, V.P. Saini, and S. Suthar, Removal of Pharmaceuticals and Personal Care Products (PPCPs) from Water by Adsorption on Aluminum Pillared Clay. *J. Porous Mat.* 27, 383–393 (2020).
- G. Chauhan, R.B. Gonzalez-Gonzalez, and H.M.N. Iqba, Bioremediation and Decontamination Potentials of Metallic Nanoparticles Loaded Nanocomposite Matrices – A Review. *Environ. Res.* 204, 112407 (2022).
- Y. Ying, S.K. Kamarudin, and M.S. Masdar, Silica-Related Membranes in Fuel Cell Application: An Overview. *Int. J. Hydrogen Energy* 43, 16068–16084 (2018).
- M.F. Samberan, M.M. Hasani-Sadrabadi, R.S. Ghaffarian, and A. Alimadadi, Investigation of the Effects of AMPS-Modified Nanoclay on Fuel Cell Performance of Sulfonated Aromatic Proton Exchange Membranes. *Int. J. Hydrogen Energy* 38, 14076–14084 (2013).
- F. Altaf, R. Batool, R. Gill, Z. UrRehman, H. Majeed, A. Ahmad, M. Shafiq, D. Dastan, G. Abbas, and K. Jacob, Synthesis and Electrochemical Investigations of ABPBI Grafted Montmorillonite Based Polymer Electrolyte membranes for PEMFC Applications. *Renew. Energ.* 164, 709–728 (2021).
- J. Niu, W. Zhang, S. Li, W. Yan, X. Hao, Z. Wang, F. Wang, G. Zhang, and G. Guan, An Electractive Montmorillonite/Polyaniline Nanocomposite Film: Superfast Ion Transport And Ultra-Affinity Ion Recognition for Rapid and Selective Separation of Pb²⁺ Ions. *Chem. Eng. J.* 413, 127750 (2021).
- R. Batra and R. Purwar, Deduction of a Facile Method to Construct Antheraea Mytila Silk Fibroin/Gelatin Blend Films for Prospective Biomedical Applications. *Polym. Int.* 70, 73–82 (2021).
- Z. Fu, J. Liu, and Q. Liu, SPEEK/PVDF/PES Composite as Alternative Proton Exchange Membrane for Vanadium Redox Flow Batteries. *J. Electron. Mater.* 45, 666–671 (2016).
- W. Mabrouk, L. Ogier, S. Vidal, C. Sollogoub, F. Matoussi, and J.F. Fauvarque, Ion Exchange Membranes Based Upon Crosslinked Sulfonated Polyethersulfone for Electrochemical Applications. *J. Membrane Sci.* 452, 263–270 (2014).
- W. Mabrouk, R. Lafi, K. Charradi, L. Ogier, A. Hafiane, J.F. Fauvarque, and C. Sollogoub, Synthesis and Characterization of New Proton Exchange Membrane Deriving from Sulfonated Polyether Sulfone using Crosslinking for Electrodialysis Applications. *Poly. Eng. Sci.* 60, 3149–3158 (2020).
- W. Mabrouk, R. Lafi, J.F. Fauvarque, A. Hafiane, and C. Sollogoub, New Ion Exchange Membrane Derived from Sulochlorated Polyether Sulfone for Electrodialysis Desalination of Brackish Water. *Polym. Advan. Technol.* 32, 304–314 (2021).

29. L. Wang, L. Dou, and G. Guan, Preparation of Sulfonated Poly(Aryl Ether Sulfone) Electrospun Mat/Phosphosilicate Composite Proton Exchange Membrane. *J. Electron. Mater.* 46, 1883–1888 (2017).
30. B. Tyagi, C.D. Chudasama, and R.V. Jasra, Characterization of Surface Acidity of an Acid Montmorillonite Activated with Hydrothermal, Ultrasonic and Microwave Techniques. *Spectrochim. Acta Part A* 64, 273–278 (2006).
31. V. Yadav, N. Niluroutu, S. Bhat, and V. Kulshrestha, Sulfonated Poly(Ether Sulfone) Based Sulfonated Molybdenum Sulfide Composite Membranes: Proton Transport Properties and Direct Methanol Fuel Cell Performance. *Mater. Adv.* 1, 820 (2020).
32. E. Günster, D. Pestreli, C.H. Ünlü, O. Atici, and N. Güngör, Synthesis and Characterization of Chitosan-MMT Biocomposite Systems. *Carbohydr. Polym.* 67, 358–365 (2007).
33. R. Gosalawit, S. Chirachanchai, S. Shishatskiy, and S.P. Nunes, Sulfonated Montmorillonite/Sulfonated Poly(Ether Ether Ketone) (SMMT/SPEEK) Nanocomposite Membrane for Direct Methanol Fuel Cells (DMFCs). *J. Membrane Sci.* 323, 337–346 (2008).
34. Z. Gaowen and Z. Zhentao, Organic/Inorganic Composite Membranes for Application in DMFC. *J. Membrane Sci.* 261, 107–113 (2005).

Publisher's Note Springer Nature remains neutral with regard to jurisdictional claims in published maps and institutional affiliations.